Journal of Engineering Research and Reports

9(2): 1-14, 2019; Article no.JERR.53495
ISSN: 2582-2926

Punching Strengthening of Concrete Slab-column Connections Using Near Surface Mounted (NSM) Carbon Fiber Reinforced Polymer (CFRP) Bars

Ahmed H. Abdel-Kareem[1*]

[1]Department of Civil Engineering, Benha Faculty of Engineering, Benha University, Egypt.

Author's contribution

The sole author designed, analysed, interpreted and prepared the manuscript.

Article Information

DOI: 10.9734/JERR/2019/v9i217013
Editor(s):
(1) Dr. Grzegorz Sierpiński, Associate Professor, Department of Transport Systems and Traffic Engineering, Silesian University of Technology, Poland.
Reviewers:
(1) Shashidhar K. Kudari, CVR College of Engineering, India.
(2) Jianhui Yang, Henan Polytechnic University, China.
Complete Peer review History: http://www.sdiarticle4.com/review-history/53495

Original Research Article

Received 20 October 2019
Accepted 23 December 2019
Published 01 January 2020

ABSTRACT

This paper investigates experimentally the effect of near surface mounted (NSM) carbon fiber reinforcement polymer (CFRP) bars as externally strengthening on the punching shear behavior of interior slab-column connections. Many researchers used NSM as a novel strengthening technique in various structural elements. However, the strengthening of slab-column connections using NSN is relatively new. Seven Reinforced concrete (RC) square slabs with a concentric column were tested over simply supported four sides. One control specimen was tested without strengthening, four specimens were strengthened using NSM-CFRP bar installed in pre-cut groove surrounded the column at the tension side of the slab, and two specimens were strengthened using externally bonded (EB) CFRP strips which have the same tensile force of the CFRP bars. The arrangement and the location of the strengthened materials were also test variables. The test results showed that using NSM strengthening technique significantly increased the punching shear capacity and ultimate stiffness compared to using EB strengthening technique. Where the increasing in the punching capacity and ultimate stiffness were 18% and 13-18%, respectively. Moreover, the NSM-CFRP bars greatly reduced the cracks in the punching shear zone around the columns. The measured ultimate punching shear capacity for the tested specimens showed very reasonable agreement with the calculated punching loads based on an analytical model for slab-column connections strengthened using FRP that account for its arrangement and location.

**Corresponding author: Email: ahmed.abdelkareem@bhit.bu.edu.eg;*

Keywords: Slab-column; punching shear; strengthening; near surface mounted; CFRP; external bonded.

1. INTRODUCTION

Flat slabs have been extensively used in a variety of construction projects. Structural system without dropped beams results in increasing floor height, easy formwork and speedy construction. In this system, the punching shear failure of slab-column connections is the most critical part. The natural of punching shear failures are brittle and occur within small deflections. Where, the slab punching strength can become insufficient for several reasons, such as design / construction errors, change of building use, new installations of a service which require openings in the slab and corrosion of reinforcement. These issues provide the need of strengthening existing slab-column connections.

Over the past decade, research studies have been conducted on using fiber reinforcement polymers (FRP) as strengthening material to improve the performance of existing slab-column connections. FRP can be used in two methods; externally installed [1-6] and internally installed [7-10]. The FRP externally strengthened system consists of one or more FRP sheets / laminates bonded to the tension side of the slab using epoxy adhesive. This strengthening method increase the flexural reinforcement and therefore increase the punching shear strength by delaying the shear cracks formation. The common failure for external strengthening technique is the premature debonding of FRP, which could be delayed and improve the structural behavior of strengthened connection by providing end anchorage to the externally bonded FRP [11]. Post-installation of FRP studs or FRP shear dowels, as shear reinforcement, in drilled holes filled with suitable epoxy grout falls into internal strengthened method for slab-columns connections. The drilled holes, to insert shear reinforcement, in the critical punching shear area of the slab near the column could further damage the degenerated slab. This strengthening technique is not practically the suitable solution in several situations.

The near surface mounted (NSM) for strengthening RC elements is the recent and promising technique. In this strengthening method, grooves are cut in the concrete cover of the structural elements, and are partially filled by a suitable bonding adhesive. After that, the reinforcing bars are inserted in the grooves and covered by the bonding adhesive. Finally, the surface of the structure element is levelled. The NSM technique has several advantages compared with externally bonded (EB) technique. Debonding problems in EB technique is less in NSM technique, which led to improvement in the structural behavior of strengthened elements. In addition, the concrete cover and adhesive material protect the reinforcing bars from temperature, vandalism, and damage. Several researches investigated the rehabilitation and strengthening of RC beams and slabs in flexure by NSM technique using FRP bars [12-16]. Another researches investigated the shear performance of RC beams strengthened by the NSM technique using FRP bars in the form of external stirrups [17-20]. To the knowledge of the author, there is no researches that have been conducted on using NSM technique in strengthening slab-column connections.

The aim of this research is to assess the efficiency of NSM technique using carbon FRP (CFRP) bars in strengthening the slab-column connections against punching shear failure. The carried-out tests on the slab-column specimens are described and the most important outcomes are showed and analyzed. Also, the experimental results are compared with the results obtained from an analytical model.

2. EXPERIMENTAL PROGRAM

2.1 Specimens and Text Matrix

Seven RC slab-column connections subjected to punching loading were constructed and tested in the experimental program. The main objective of the test program was to investigate the behavior of RC slab-column connections strengthened at tension side of the slab using NSM technique. One un-strengthened specimen was intended to serve as control specimen. Four specimens were strengthened using NSM-CFRP bar of 10 mm diameter with different arrangements and locations. The remaining two specimens were strengthened using CFRP strips externally bonded to the tension side of the slab, with two different strengthening arrangements similar to that used on NSM strengthened specimens for comparison purposes. Also for comparison, the width of CFRP strip was chosen to give total tension force for CFRP strip similar to that of CFRP bar.

The description of strengthening schemes and nomenclatures for tested specimens are gives in Table 1. The first letter of the nomenclature of the specimen (S) standing for slab. The second letter points to the strengthening technique, where (B) for NSM-CFRP bar and (S) for CFRP strips externally bonded. The third letter refers to the strengthening configuration relative to the orientation of the slab reinforcement, (O) for orthogonal and (S) for skewed. The last number indicates the distance of centerline of the NSM-CFRP bar or CFRP strip to the column face, where (0.5) for distance equal half the slab depth and (1.0) for distance equal the slab depth. Fig. 1 shows the strengthening schemes used in the presents study.

All the specimens had the same dimensions and steel reinforcement details, as shown in Fig. 2. The slab dimensions were 1100x1100 mm and 130 mm thick. The specimens were designed to be supported along the four edges with clean spans 1000 mm in both directions. A column stub 150x150 mm was cast monolithically at the center of the slab. To simulate the actual interior slab-column connections, the column extended 150 mm up and 50 mm down the slab faces, and the slab reinforced with top and bottom meshes. The slabs were reinforced using high tensile steel bars of 10 mm diameter. The bottom mesh was 11Ø10 and the top mesh was 7Ø10. The columns were reinforced with vertical high tensile steel bars Ø12 in each corner of the column and normal mild steel stirrups 8 mm every 100 mm. The grooves required to install CFRP bars in the specimens strengthened using NSM technique were formed by square wood pieces (25x25 mm) fixed at the bottom of the molds, with required shapes, before pouring concrete. A clear concrete cover of 30 mm and 15 mm was kept at bottom and top of the slabs, respectively.

Table 1. Test matrix

Specimen code	Strengthening technique	Strengthening configuration	Location from* column
Control			
S-B-O-0.5	NSM-CFRP bar	Orthogonal	d**/2
S-B-O-1		Orthogonal	d
S-B-K-0.5		Skewed	d/2
S-B-K-1		Skewed	d
S-S-O-0.5	FB-CFRP strips	Orthogonal	d/2
S-S-K-0.5		Skewed	d/2

*Distance between center line of CFRP bar or CFRP strip to the column face; **Slab depth

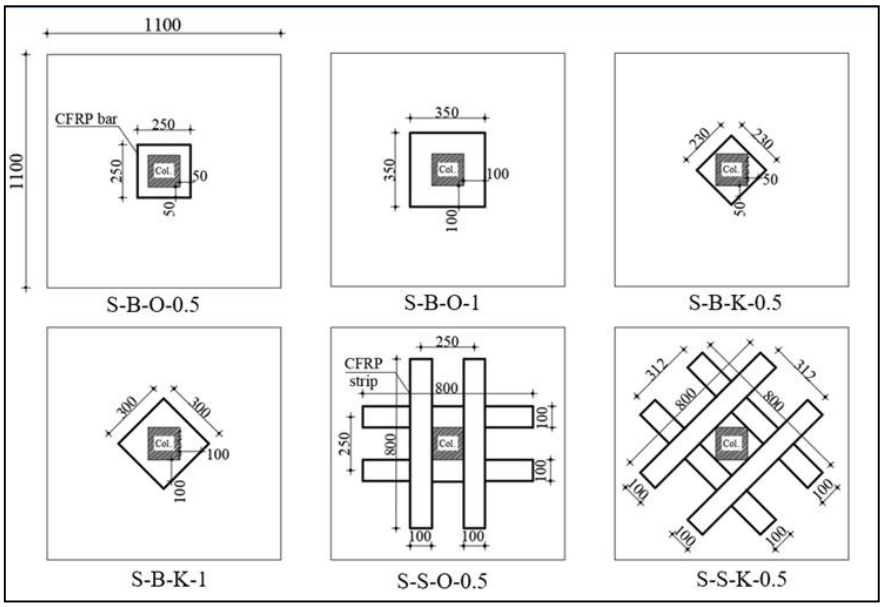

Fig. 1. Strengthening schemes (All dimensions in mm)

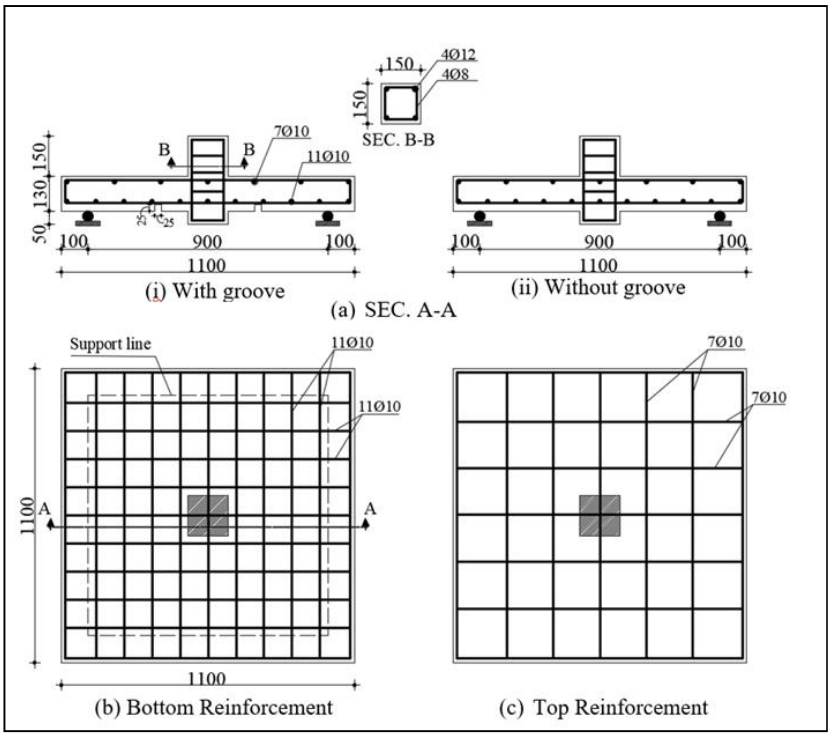

Fig. 2. Dimensions and reinforcement details for tested specimens (All dimensions in mm)

2.2 Material Properties

2.2.1 Concrete

The concrete mixture used in the tested specimens consists of Ordinary Portland Cement (OPC-42.5 grade), natural sand with 2.6 fineness moduli and crushed dolomite with maximum aggregate size 16 mm. the target compressive strength (f_{cu}) at 28 days was 35 Mpa. The actual f_{cu} was obtained at the day of testing and based on cubes (150x150x150 mm) were casted and cured with the tested specimens.

2.2.2 CFRP bars

CFRP bars were locally fabricated using pultrusion process, and formed similar to the shapes of the grooves in the bottom face of the specimens, as shown in Fig. 3. The bars are made of carbon fibers with resin from polyester polymer. A specimen of the CFRP rod was tested to obtain the mechanical properties, which shows in Table 2.

2.2.3 CFRP strips

CFRP strips used in this study are SikaWrap-230, which is a product of Sika Company. The strips were bonded to the bottom face of the slabs using epoxy Sikadur-330. Table 2 gives the mechanical properties of the carbon fiber, according to the manufacturer. The width of the strips was 100 mm, and determined to give the same tension force of CFRP bar.

2.3 Strengthening Procedures

2.3.1 NSM strengthening technique

The grooves at the tensioned side of the slabs were formed during concrete casting using wood pieces, as indicated previously. After casting and curing the specimens, the grooves were cleaned from the wood pieces and loose materials. Then the epoxy Sikador-330 filled half way the groove, CFRP bar was slightly inserted forcing the epoxy to fill completely between the sides of the groove and the bar. A second layer of epoxy was applied to fill the groove and the residue epoxy were removed, and the surface was leveled. Fig. 4 shows the strengthening procedures for a specimen using NSM technique.

2.3.2 EB strengthening technique

The CFRP strips, externally strengthened the concrete slab, were cutoff 800 mm long and 100 mm width and were placed around column in an

orthogonal or skew orientation, as shown in Fig. 1. Angle grinder with a wire brush was used to rough the concrete surface, where the CFRP strips would be placed. The surface was cleaned from loose materials using a vacuum cleaner. Then, the epoxy adhesive (Sikadur-330) was applied on both CFRP strips surfaces and the marked locations on the concrete surface. The strips were then pressed on to the concrete surface using a smaller roller. The excess epoxy was squeezed from the slides and cleaned.

2.4 Test-up and Instrumentation

The specimens were centrally loaded using a hydraulic jack, 1000 kN maximum capacity, connected to an electric pump, and hanged in a rigid reaction frame, 1000 kN maximum capacity. The specimens were supported on steel rod bars along all four sides to behave as simply supported. The rod bars were welded to I-shaped steel beams. The load was distributed to the head of column stub using a thick steel plate. The applied load was record using a load cell of 1000 kN maximum capacity placed under the hydraulic jack. To monitor the deflection, five Linear Variable Differential Transducers (LVDT) were placed beneath the center of the column stub and quarter-span of the slab in the two directions. For each strengthened specimen, one strain gauge was attached to the CFRP bar or mid-point of the CFRP strip. The cracks propagation were marked with applied load increasing up to failure. All test data were captured using data acquisition system and recorded on a computer at intervals of two seconds. Fig. 5 illustrates the test set-up.

Fig. 3. CFRP bars used in this study

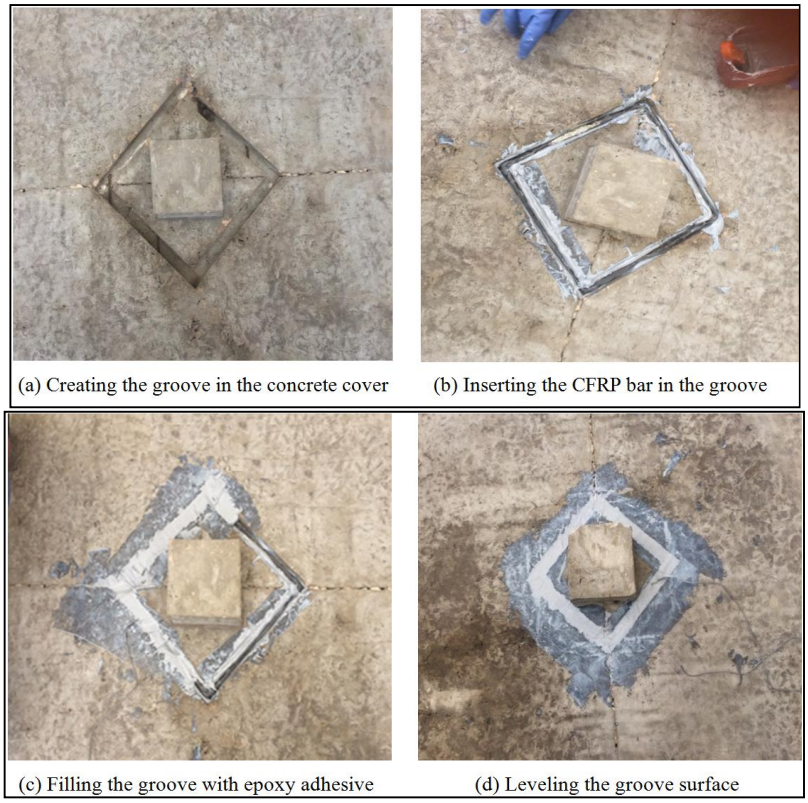

Fig. 4. Strengthening procedures using NSM technique

Table 2. Dimensions and characteristic properties of CFRP

a) CFRP bars		b) CFRP strips	
Property		**Property**	
Diameter of bars (mm)	10	Fabric design thickness (mm)	0.128
Area of bars (mm^2)	78.5	Fabric width (mm)	100
Area of fibers (mm^2)	29.3	Tensile strength (MPa)	4300
Fiber ratio by area	37%	Elasticity modulus (MPa)	234000
Tensile strength (MPa)	1420	Strain at failure	1.84%
Elasticity modulus (MPa)	216000		
Strain at failure	$6600x10^{-6}$		

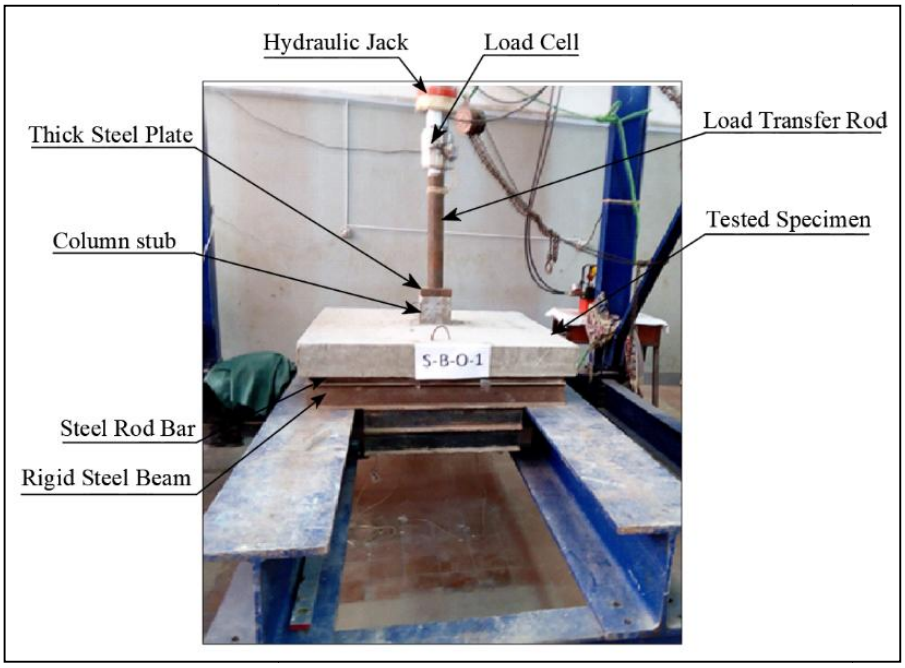

Fig. 5. Test set-up

3. EXPERIMENTAL RESULTS AND DISCUSSION

The experimental test results are summarized in Table 3. The effect of test parameters on the behavior of tested specimens under punching load will been discussed in the following sections.

3.1 Load-deflection Relationships

Figs. 6-8 shows the deflection of the column stub, located at the center of the slab, versus the applied load according to the test parameters. It can be seen that the curve of control specimen increased almost linear till reached the peak load, and then the load suddenly dropped due to brittle punching shear failure. The load-deflection curves for the strengthened specimens were similar to that of control specimen, except the decreasing of the load after reaching its peak value was less sharp. The load-deflection plots show increasing in the ultimate load and decreasing in the deflection at the same load for all strengthened specimens compared to the control specimen. The reduction of the deflection of the strengthened specimens compared to control specimen were qualified by measuring the deflection for all test specimens at the ultimate load of the control specimen (Δ_{uc}), which listed in Table 3 and calculated the deflection ratio of the strengthened specimens to the control specimen ($\Delta_{uc/}\ \Delta_{uc,c}$), which is also listed in the same table. The reduction in the deflection of the strengthened specimens ranged from 50% to 74% compared to the control specimen, which indicate increasing in the stiffness of the strengthened specimens.

Table 3. Summary of experimental results

Specimen code	f_{cu} (Mpa)	1st Cracking		Ultimate		Δ_{uc}*	$\frac{P_u}{P^{**}_{u,c}}$	$\frac{\Delta_{uc}}{\Delta^{***}_{uc,c}}$	Un-cracked stiffens (K_i)	Ultimate stiffness (k_U)
		Load (P_{cr}) (kN)	Cracking Δ_{cr} (mm)	Load (P_u) (kN)	Cracking Δ_u (mm)				$\frac{P_{cr}}{\Delta_{cr}}$ (kN/mm)	$\frac{(P_u - P_{cr})}{(\Delta_u - \Delta_{cr})}$ (kN/mm)
Control	32.8	73	3.35	222.68	10	10	1	1	21.79	22.5
S-B-O-0.5	33.4	81	2.3	311.14	10.5	6.39	1.4	0.64	35.22	28.07
S-B-O-1	31.9	88	2.17	338.56	9.19	5.56	1.52	0.55	40.55	35.69
S-B-K-0.5	34.3	94	2.4	326.07	10.0	5.87	1.46	0.58	39.16	30.53
S-B-K-1	32.1	98	2.26	347.82	9.1	5.07	1.56	0.51	43.36	36.52
S-S-O-0.5	32.4	72	2.1	263.50	9.8	7.42	1.18	0.74	34.3	24.87
S-S-K-0.5	35.8	79	2.0	277.50	9.64	7.03	1.25	0.70	39.5	25.98

* *Deflection of tested specimens at P_u of control specimen;* ** *P_u of control specimen;* *** *Deflection of control specimen corresponding to its P_u*

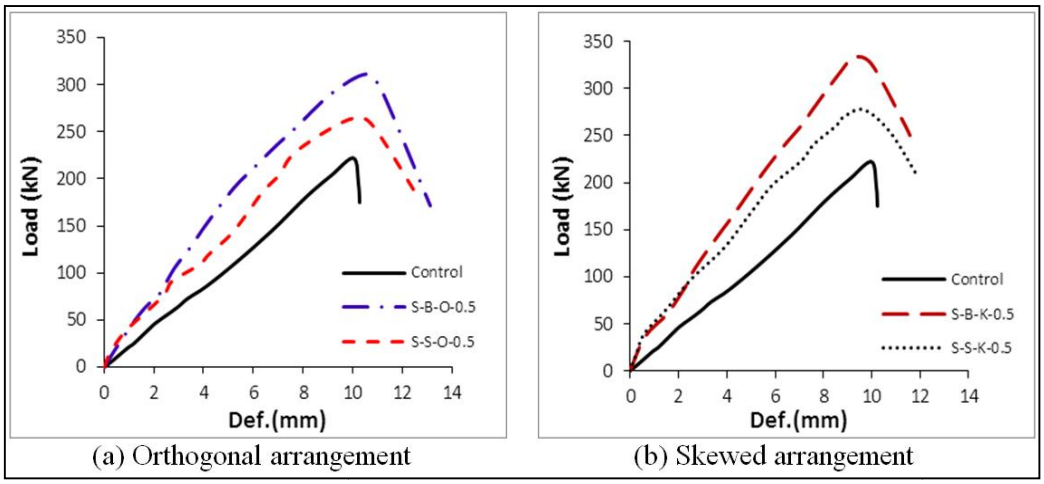

Fig. 6. Central deflection comparison based on the strengthening techniques

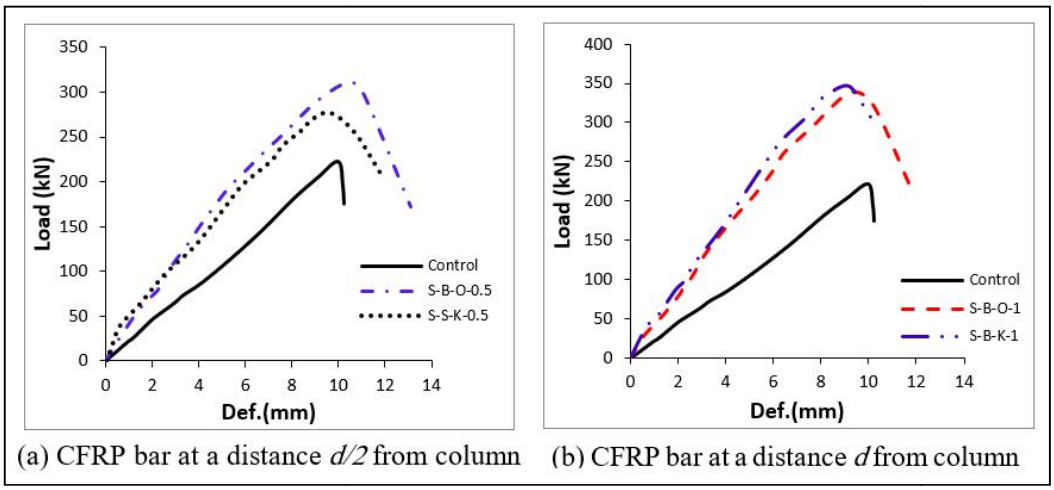

Fig. 7. Central deflection comparison based on the strengthening arrangements

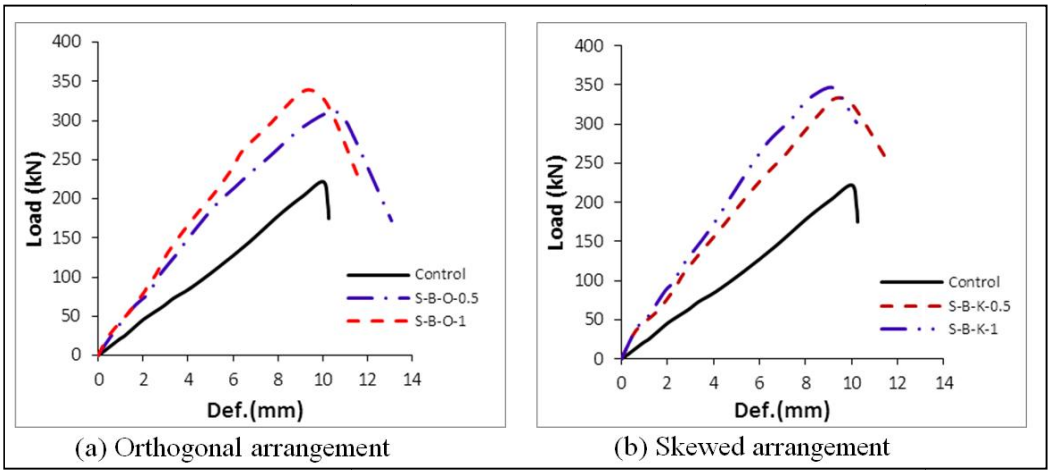

Fig. 8. Central deflection comparison based on the strengthening locations

3.2 Load Carrying Capacity

The cracking load (P_{cr}), the ultimate load (P_u), and the gain in the P_u for the strengthened specimens compared with the control specimen are listed in Table 3. P_{cr} for the specimens strengthened externally by CFRP strips was slightly improved in comparison with the control specimen. On the other hand, the strengthening using NSM-CFRP bar effectively enhanced P_{cr}, where it increased in comparison with the control specimen by 11-20% and 29-34% for orthogonal and skewed bars respectively. The ultimate load capacity for all strengthened specimens had a notable increase, where the gain in P_u was 18-56%. The increase in P_u for the specimens strengthened with NSM-CFRP bar over the control specimen was 40-56%. While the increase in *Pu* was only 18-25% for specimens strengthened with EB-CFRP strips. Thus, it can been concluded that using NSM technique for strengthening slabs has well-contributed in increasing the punching shear capacity of slab-column connections than using EB technique.

Considering the strengthening arrangement, it can be noted that the skewed strengthening arrangement produced a slight increase in P_u, compared to the orthogonal arrangement, and that was for specimens strengthened using either EB technique or NSM technique. The increasing in P_u for specimens with skewed strengthening arrangement was 5.9-2.6% more than that with orthogonal arrangement.

Comparing the different locations of CFRP bar from the column face, it can be noted that the bar placed at a distance equal to the slab depth, *d*, from the column face gave relatively higher increase in P_u compared to the bar placed at a distance *d*/2. For specimens with orthogonal strengthening arrangement, specimen S-B-O-1 with bar at a distance *d* from the column face had 8.8% increase in *Pu* than specimen S-B-O-0.5 with bar at a distance *d*/2. Similar, for the specimens with skewed strengthening arrangement, specimen S-B-K-1 has 6.7% increase in P_u than specimen S-B-K-0.5. Fig. 9 shows a comparison between P_{cr} and P_u for all tested specimens.

3.3 Stiffness

The un-cracked stiffness (K_i) and the ultimate stiffness (K_u) had been calculated for tested specimens from the load and deflection values at cracking and ultimate loads, as presented in Table 3. It shows k_i increased significantly for all strengthened specimens by 57-99% compared to the control specimen. On the other hand, k_u affected by the strengthening technique. Where, k_u effectively increased for specimens strengthened using NSM-CFRP bar by 25-62%, and slightly increased for specimens with EB-CFRP strips by 11-15% compared to the control specimen.

Considering the effect of strengthening arrangement, the skewed strengthening arrangement showed higher stiffness compared to the orthogonal arrangement. Where, K_i and K_u for the specimens with skewed strengthening arrangement increased by 7-15% and 4-9%, respectively compared to the specimens with orthogonal arrangement. These results indicate that K_u was less affected by strengthening arrangement than K_i. On the contrary, the effect of the location of CFRP bar from the column face on K_i was less than K_u. Where, the specimens with CFRP bar located at a distance *d* from the column face, *Ki* and *Ku* increased by 11-15% and 20-27%, respectively than that with CFRP bar located at a distance *d*/2.

3.4 Crack Propagation and Failure Characteristics

Cracking pattern and distribution at failure at the bottom face of the slabs for all tested specimens are shown in Fig. 10. The failure mode for all specimens was punching shear. The control specimen exhibited flexural cracks that started near the column stub and extended towards the slab edges, especially towards the corners as the applied load increased. The failure was sudden, immediately after the specimen reached its ultimate capacity, and followed by a sharp drop in the load exerted to the control specimen. The punching shear failure plane on the bottom face can be easily seen around the column and at distances from the its face ranged from 180 mm to the slab edges (425 mm), and associated with separation from the slab surface.

For the NSM strengthened specimens, the flexural cracks started outside the strengthened CFRP bar when the bar located at a distance *d*/2 from the column face, or flexural cracks started near the column face and did not propagate through the strengthened bar when the bar

located at *d* from the column face. Similar to the control specimen, the flexural cracks propagated towards the slab edges. Reducing the spread of flexural cracks in the punching shear zone around the columns led to an increase in the punching shear capacity for the specimens. The distances from punching shear failure planes to the columns face were less than that for control specimen; especially for specimens strengthened with NSM bar at a distance *d* form the column.

The specimens strengthened using EB-NSM strips suffered from premature debonding of CFRP strips. As the load increased, some of CFRP strips debonded from the bottom face of the slab, and pulled away from the specimen with the concrete cover. At failure, strips debonded from the slab as the truncated concrete cone was pushed through the slab. Due to the CFRP strips covered the zone around the column, the cracks at bottom face of the slabs were invisible.

4. CALCULATED PUNCHING SHEAR CAPACITY

The predicted punching shear capacity of the slab-column connections strengthened with CFRP was obtained using the analytical model developed by Harajli and Soudki [21]. This model is based on that the punching capacity of slab-column connection increased with the increase in the flexural capacity of the slab. The FRP either NSM bars or EB strips is considered as additional reinforcement in the flexural capacity. For the FRP strengthened slab, the average moment capacity per unite width (*m*) was derived from the conventional equilibrium requirements for force and moment and the compatibility of strain along the depth of the slab section as follows:

$$\mathrm{m} = \rho_s f_y d^2 \left[1 - 0.59\left(\rho_s \frac{f_y}{f_c} + \rho_f \frac{K_v f_{fu}\, h/d}{f_c}\right)\right] + \rho_f k_v f_{fu} h^2 \left[1 - 0.59\left(\rho_s \frac{f_y d/h}{f_c} + \rho_f \frac{k_v f_{fu}}{f_c}\right)\right] \quad (1)$$

$$\rho_s = \frac{A_s}{wd}, \qquad \rho_f = \frac{A_f}{wh} \quad (2)$$

Where ρ_s and ρ_f are the reinforcement ratio of the tension steel of the slab and FRP reinforcement either NSM bars or EB strips, respectively; A_s is the area of the tension steel per slab width *w;* A_f is the area of FRP bars or strips; *h* is the slab height; f_y is the yield strength of steel reinforcement; f_c is the cylindrical concrete compressive strength= $0.8f_{cu}$; and K_v is a factor which accounts for the ratio of stress development in FRP bars or strips at ultimate capacity of the specimens to the ultimate strength f_{fu} of the bars or strips.

According to Canadian standers (CSA-06) [22], the factor K_v in Eq. (1) estimated as follows:

$$K_v = \frac{K_1 K_2 L_e}{11{,}900\varepsilon_{fu}} \leq 0.75 \quad (3)$$

In which K_1 and K_2 are factors which represent for the concrete strength and wrapping method, respectively, and L_e is the active bond length, where the bond stress is maintained. The factors are given as:

$$K_1 = \left(\frac{f_c'}{27}\right)^{\frac{2}{3}} \quad (4)$$

$$K_2 = \frac{L_f - 2L_e}{L_f} \quad (5)$$

$$L_e = \frac{25{,}350}{(t_f E_f)^{0.58}} \quad (6)$$

Table 4. Comparison of experimental and predicted results

Specimen Code	$P_{u,exp}$ (kN)	$P_{u,calc}$ (kN)	$\frac{P_{u,calc}}{P_{u,exp}}$
S-B-O-0.5	311.14	292.82	0.94
S-B-O-1	338.56	303.35	0.90
S-B-K-0.5	326.07	298.36	0.92
S-B-K-1	347.82	311.19	0.89
Mean			0.91
Standard deviation			0.02
S-S-O-0.5	263.5	282.27	1.07
S-S-K-0.5	277.5	282.9	1.02
Mean			1.05
Standard deviation			0.04

Where, L_f is the dimension of the slab in the direction of FRP bars or strips; t_f is the thickness of FRP strip or the diameter of FRP bar; and E_f is the elasticity modulus of FRP either bar or strip.

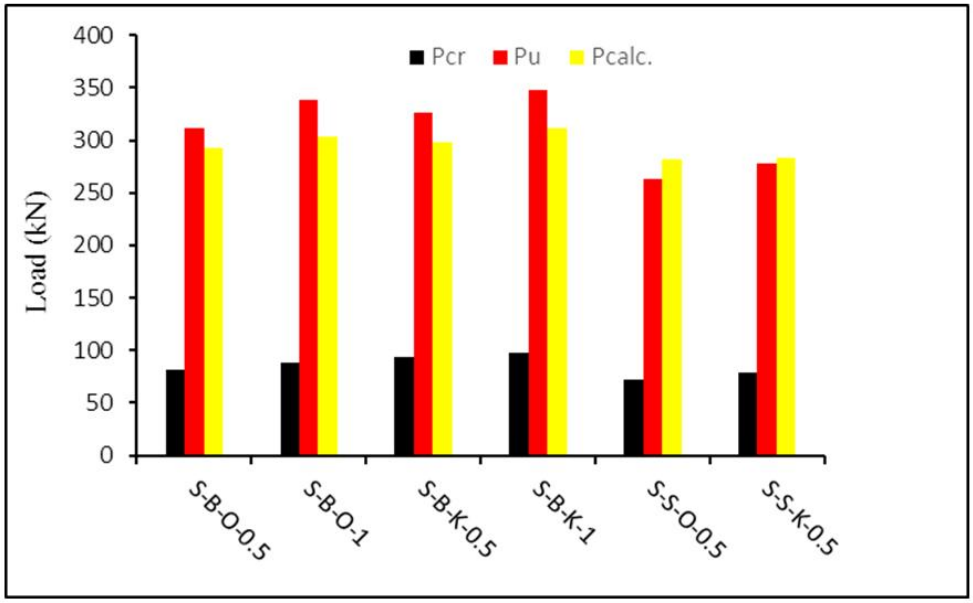

Fig. 9. Comparison between cracking load, experimental ultimate load and calculated ultimate load for the strengthened specimens

The area of FRP bars or strips was modified by Sharaf, et al. [23] to include the effect of the strengthening schemes, amount and spacing of FRP bars or strips as follows:

$$A_f = \sum_{i=1}^{n} \frac{\eta}{\xi} b_{fi} t_{fi} \quad (7)$$

$$\eta = \Delta \cos\theta \quad (8)$$

$$\xi = \frac{\sum_{i=1}^{n} \frac{b_{fi}}{s_i}}{n} \quad (9)$$

In which η is a factor which accounts for the effect of the orientation of FRP bars or strips; θ is the orientation of FRP to the slab reinforcement; Δ is considered 1 for orthogonal strengthening and 2 for skewed strengthening; and ξ is a factor that accounts for the effect of FRP locations relative to the column face, the spacing between FRP bars or strips and the number of FRP bars or strips; b_f is the width of FRP strip or the diameter of FRP bar; s is the distance from the center of each FRP bar or strip to the column face; and n is the number of FRP bars or strips per slab width.

The flexural capacity of the slab can be estimated from the average moment capacity per unite width (m) using yield line analysis (Elsner and Hognestad [24]) as follows:

$$P_{flex} = 8m\left(\frac{1}{1-r/w} - 3 + 2\sqrt{2}\right) \quad (10)$$

Where r is the width of a column or the side length of a loaded area.

Mowrer and Vanderbilt [25] proposed equation to estimate the punching shear strength (P_u) of a flat slab as follows:

$$P_u = \frac{0.8(1+d/r)bd\sqrt{f_c'}}{1+(0.4\ 33bd\sqrt{f_c'}/P_{flex})} \quad (11)$$

In which b is the perimeter of the column or the loaded area.

The predicted punching shear capacity for the tested specimens calculated according to Eqs. (1)-(11) were compared with the experimental results as shown in Table 4 and Fig. 9. From comparison, it can be concluded that the proposed analytical model gave slightly under estimate for NSM-CFRP strengthened specimens as the average ratio $P_{u.calc}/P_{u.exp}$ is 0.91 with a coefficient of variation of 0.02. While the predicted punching shear capacity of EB-CFRP strengthened specimens were slightly overestimate as the average ratio $P_{u.calc}/P_{u.exp}$ is 1.05 with a coefficient of variation 0.04.

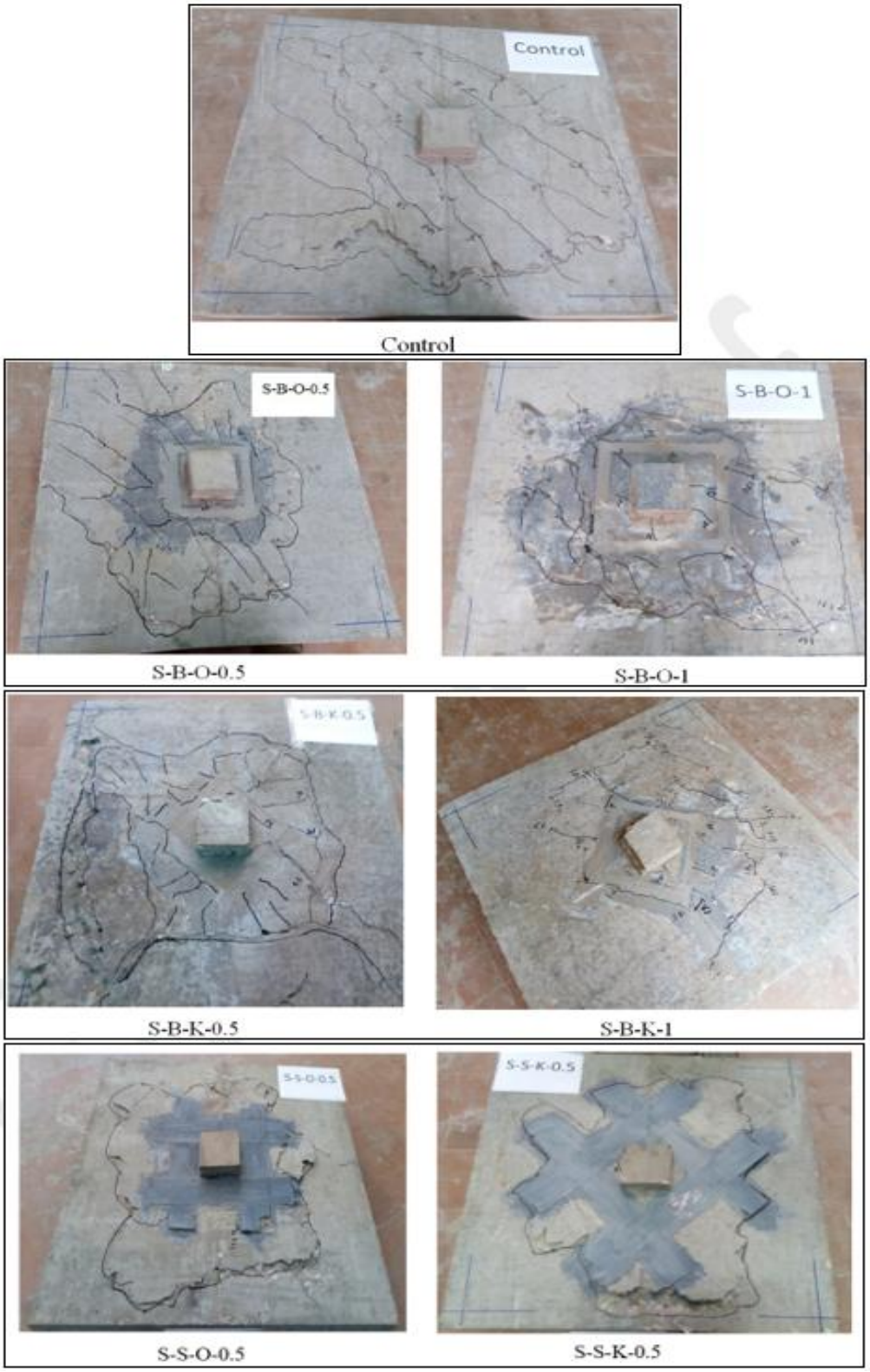

Fig. 10. Crack patterns at failure load for the tested specimens (bottom faces)

5. SUMMARY AND CONCLUSION

In this study, NSM technique were used to strengthen slab-column connections against punching shear failure. A CFRP bar was installed surrounding the column at the bottom face of the slab. A total of seven square slabs with a concentric column were constructed and tested up to failure, one control specimen without strengthening, four specimens strengthened using NSM-CFRP bar and two specimens strengthened using CFRP strips externally bonded to the bottom face of the slab. For comparison purposes, the width of the CFRP strip was chosen to have the same tensile force of the CFRP bar. For the considered strengthening techniques, the test variables were the strengthening arrangement relative to the orientation of the slab reinforcement and the strengthening location to the column face. Based on this investigation, the following conclusions may be drawn:

1. The ultimate punching capacity was significantly increased for the specimens strengthened using NSM technique over that strengthened using EB technique. Comparing with the control specimen, the punching capacity increased by 40-56% for specimens strengthened with NSM-CFRP bar and increased by 18-25% for specimens strengthened with EB-CFRP strips.
2. The stiffness of all strengthened specimens increased in un-cracked stage in the range from 57% to 99% than the control specimen. The stiffness in cracked stage was affected by the strengthening technique. Where, comparing with the control specimen the ultimate stiffness increased greatly by 25-62% for specimens strengthened using NSM-CFRP bar. While, the increasing in ultimate stiffness was 18-25% for specimen strengthened using EB-CFRP strips.
3. Installing the CFRP bar on at a distance equal the slab depth, *d*, from the column face gave higher punching capacity and cracking stiffness than installing the bar at a distance *d*/2.
4. Strengthening using skewed arrangement showed a slight enhancement in the punching capacity and cracking stiffness compared to the orthogonal arrangement.
5. All tested specimens failed in punching shear mode. For the specimens strengthened using NSM-CFRP bar, the cracks in the punching shear zone around the columns reduced which led to increasing in the punching capacity of the specimens. Where, the cracks started outside the strengthened CFRP bar when the bar located on a distance *d*/2 from the column face, or cracks started near the column face and did not propagated through the strengthened bar when the bar located at *d* from the column face. The specimens strengthened using EB-CFRP strips suffered from premature debonding of the strips.
6. The analytical model used in this research for predicting the ultimate punching shear capacity for slab-column connections strengthened with FRP, which consider the arrangement and the location of FRP showed good agreement with the experimental results. The predicted punching shear load for strengthened specimens using NSM-CFRP bar was under estimate with an average 9% compared to the test results. While for specimens strengthened using CFRP strips, the predicated punching shear load was over estimate with an average 5%.

COMPETING INTERESTS

Author has declared that no competing interests exist.

REFERENCES

1. Malalanayake MLVP, Gamage JCPH, Silva MAL. Experimental investigation on enhancing punching shear capacity of flat slabs using CFRP. 8th International Conference on Structural Engineering and Construction Management (ICSECM2017), Kandy, Sri Lanka; 2017.
2. Abdullah A, Bailey CG, Wu ZJ. Tests investigating the punching shear of a column slab connection strengthened with non-prestressed or prestressed FRP plates. Constr Build Mater. 2013;48:1134–44.
3. Silva MAL, Gamage JCPH, Fawzia S. Performance of slab-column connections of flat slabs strengthened with carbon fiber reinforced polymers. Case Studies in Constr Mater. 2019;11.
4. Dissanayaka RHM, Silva MAL, Magallagoda LPG, Gamage JCPH. Physical behavior of CFRP retrofitted reinforced concrete slab-column connections. 9th International Conference on Sustainable Built Environment (ICSBE2018), Kandy, Sri Lanka; 2018.

5. Esfahani MR, Kianoush MR, Moradi AR. Punching shear strength of interior slab–column connections strengthened with carbon fiber reinforced polymer sheets. Eng Struct. 2009;31(7):1535–1542.
6. Soudki K, El-Sayed A, Vanzwol T. Strengthening of concrete slab-column connections using CFRP strips. J King Saud Univ Eng Sci. 2012;24(1):25–33.
7. Askar H. Repair of R/C flat plates failing in punching by vertical studs. Alexand Eng J. 2015;54(3):541–50.
8. Meisami HM, Davood M, Hikaru N. Punching shear strengthening of two-way flat slabs with CFRP grids. J Compos Constr. ASCE. 2014;18.
9. Inácio M, Ramos A, Faria D. Strengthening of flat slabs with transverse reinforcement by introduction of steel bolts using different anchorage approaches. Eng Struct. 2012; 44:63–77.
10. Ruiz M, Muttoni A, Kunz J. Strengthening of flat slabs against punching shear using post-installed shear reinforcement. ACI Struct J. 2011;434–42.
11. Hikmatullah A, Ted D, Diana P. Strengthening of slab-column connection against punching shear failure with CFRP laminates. Compos Struct. 2019; 208.
12. Sharaky IA, Torre L, Sallam HE. Experimental and analytical investigation into the flexural performance of RC beams with partially and fully bonded NSM FRP bars/strips. Compos Struct. 2015;122:113–126.
13. Sharaky IA, Torres L, Comas J, Barris C. Flexural response of reinforced concrete (RC) beams strengthened with near surface mounted (NSM) fibre reinforced polymer (FRP) bars. Compos Struct. 2014; 109:8–22.
14. Almusallam TH, Elsanadedy HM, Al-Salloum YA, Alsayed SH. Experimental and numerical investigation for the flexural strengthening of RC beams using near-surface mounted steel or GFRP bars. Constr Build Mater. 2013;40:45–161.
15. Kotynia R. Bond between FRP and concrete in reinforced concrete beams strengthened with near surface mounted and externally bonded reinforcement. Constr Build Mater. 2012;32:41–54.
16. Sun ZY, Wu G, Wu ZS, Luo YB. Flexural strengthening of concrete beams with near-surface mounted steel-fiber-reinforced polymer composite bars. J Reinf Plast Compos. 2011;1529–37.
17. Abdel-kareem AH, Debaiky AS, Makhlouf MH, Abdel-baset M. Shear Strengthening of RC Beams with FRP using (NSM) Technique. Advances in Research, SCIENCEDOMAIN international. 2019; 19(4):1-20.
18. Rizzo A, De Lorenzis L. Behavior and capacity of RC beams strengthened in shear with NSM FRP reinforcement. Constr Build Mater. 2009;23(4): 1555–67.
19. Rahal KN, Rumaih HA. Tests on reinforced concrete beams strengthened in shear using near surface mounted CFRP and steel bars. Eng Struct. 2011;33(1):53–62.
20. Meysam J, Sharbatdar MK, Jian-Fei C, Farshid JA. Shear strengthening of RC beams using innovative manually made NSM FRP bars. Constr Build Mater. 2012; 36:990–1000.
21. Harajli MH, Soudki KA. Shear strengthening of interior slab-column connections using fiber reinforced polymer sheets. J Compos Constr ASCE. 2003; 7(2):145–53.
22. CSA Committee A23.3. Design of concrete structure. Canadian Standards Association. Mississauga. Ontario, Canada; 2004.
23. Sharaf MH, Soudki KA, Van Dusen M. CFRP strengthening for punching shear of interior slab-column connections. J Compo Constr ASCE. 2006;10(5);410–18.
24. Elstner RC, Hognestad E. Shearing strength of reinforced concrete slabs. ACI Journal Proceedings. 1956;53(2):29–58.
25. Mowrer RD, Vanderbilt MD. Shear strength of light-weight aggregate reinforced concrete flat plates. ACI Journal Proceedings. 1967;64(11):722–29.

Peer-review history:
The peer review history for this paper can be accessed here:
http://www.sdiarticle4.com/review-history/53495